Ocean Engineering 220 (2021) 108350

Contents lists available at ScienceDirect

Ocean Engineering

journal homepage: www.elsevier.com/locate/oceaneng

Refinement of integrated formula of wave overtopping and runup modeling

Masatoshi Yuhi [a,*], Hajime Mase [b,c,d,e], Sooyoul Kim [f], Shinya Umeda [a], Corrado Altomare [g]

[a] School of Geosciences and Civil Engineering, Kanazawa University, Kakuma-machi, Kanazawa, 920-1192, Japan
[b] Disaster Prevention Research Institute, Kyoto University, Gokasho, Uji, Kyoto, 611-0011, Japan
[c] Hydro Technology Inst., Co., Ltd., Nakanoshima, Kita-ku, Osaka, 530-6126, Japan
[d] Nikken Kogaku Co., Ltd., 6-10-1, Nishi-Shinjuku, Shijnuku-ku, Tokyo, 160-0023, Japan
[e] Toa Corporation, 3-7-1, Nishi-Shinjuku, Shinjuku-ku, Tokyo, 163-1031, Japan
[f] Center for Water Cycle, Marine Environment and Disaster Management, Kumamoto University, 2-39-1, Kurokami, Chuo-ku, Kumamoto, 860-8555, Japan
[g] Laboratori d'Enginyeria Maritima, Universitat Politècnica de Catalunya – Barcelona Tech, Calle Jordi Girona 1-3, 08034, Barcelona, Spain

ARTICLE INFO

Keywords:
Wave overtopping
Inclined seawall
Vertical seawall
Integrated formula of overtopping and runup modeling
IFORM

ABSTRACT

This study attempts to refine a model named the Integrated Formula of Wave Overtopping and Runup Modeling (IFORM) to improve the prediction performance of mean wave overtopping discharge for a broader range of installation conditions. The empirical formula describing the relation between overtopping discharge and maximum runup has been re-examined. A set of piecewise formulas is implemented in the IFORM by optimal reconstruction of coefficients depending on the magnitude of deficit in freeboard. The refined IFORM improves the tendency to underestimate the discharge in the range of relatively high freeboard conditions, while it retains the high performance of the original IFORM in the range where the crest freeboard is relatively low. The refined model's capability for overtopping prediction is validated by comparison with various existing experimental datasets for inclined/vertical seawalls installed at relatively shallow water depth or on land. The prediction accuracy is also examined by comparison with well-known overtopping formulas. Qualitative and quantitative comparisons validate that the current model is able to reproduce the experimental observations over a broad range of overtopping conditions and that the performance of the model proposed in the present study is as good as existing representative models.

1. Introduction

The frequent occurrence of violent storms related to intensified typhoon/cyclones and/or ongoing sea-level rise induced by climate change has been becoming a serious threat for coastal societies over the world. Besides, many of the structures for coastal defense have been deteriorating at an increasing rate in many developed countries. In order to renewal such aging facilities as effective countermeasures against the violent natural forces under the changing environments, it is essentially important to properly estimate wave overtopping as well as runup in a unified way over a wide range of conditions of installation and external forces. Accordingly, significant efforts have been made during the last several decades in order to develop effective design assessment tools. Representative compilation of the available prediction methods can be found in various literature (e.g., by U.S. Army Corps of Engineers (USACE), 2002; Technical Advisory Committee on Flood Defense TAW, 2002; Coastal Engineering Committee, Japan Society of Civil Engineers, 2004; EurOtop, 2007 and 2018; Coastal Development Institute of Technology CDIT, 2018).

In Europe, EurOtop manual on wave runup and overtopping was first published in 2007 (EurOtop, 2007). The prediction formulas in EurOtop (2007) was established based on the original CLASH datasets provided by the research project on Crest Level Assessment of coastal Structures by full-scale monitoring, neural network prediction and Hazard analysis on permissible wave overtopping (De Rouck et al., 2002; Verhaeghe, 2005; Van der Meer et al., 2009). Hereafter, this dataset is called as CLASH dataset for brevity. Since then the manual has been widely incorporated in practical engineering activities. Initially, the EurOtop manual focused on the seawalls installed at relatively deep water depth. More recently, in its redaction published in 2018 (EurOtop, 2018), the prediction capability has been extended based on a new EurOtop database in which a series of additional experimental datasets for cases of low freeboard is appended to the CLASH datasets. The present EurOtop database also includes the cases of structures installed on very shallow

* Corresponding author.
E-mail address: yuhi@se.kanazawa-u.ac.jp (M. Yuhi).

https://doi.org/10.1016/j.oceaneng.2020.108350
Received 14 August 2020; Received in revised form 24 October 2020; Accepted 1 November 2020
Available online 30 December 2020

water depth based on the experimental results by Altomare et al. (2016).

In Japan, the design procedure for the determination of crest levels of seawalls is based on the Technical Standards and Commentaries for Port and Harbor Facilities in Japan (TSC) issued by the Overseas Coastal Area Development Institute of Japan (2009) and the Technical Standards and Commentaries for Coastal Facilities in Japan (Coastal Development Institute of Technology CDIT, 2018). Proposed prediction methods are summarized by Coastal Engineering Committee, Japan Society of Civil Engineers JSCE (2004) in which most of the proposed methods treated the vertical and inclined seawalls separately. Using the CLASH datasets, Goda (2009b) formulated a unified prediction model for inclined/vertical seawalls to estimate the overtopping discharge. More recently, Mase et al. (2013) have developed an integrated prediction model for wave runup and overtopping to provide an effective design tool based on the consistent assessment of runup and overtopping. It was named later as IFORM (Integrated Formula of Overtopping and Runup Modeling) in Tamada et al. (2015). The model is based on an imaginary slope method proposed by Nakamura et al. (1972), and can be flexibly applied to a variety of design conditions including the complex shape of cross-sections. Moreover, the model satisfies the proper boundary conditions for overtopping formulas proposed by Hedges and Reis (1998), which can provide a unified and consistent prediction of wave runup and overtopping. Initially, IFORM was developed for gently-sloped seawalls constructed on land or very shallow water that was typically seen along the Japanese coastlines. One of the distinct features of IFORM is that the model application is straightforward even in cases of seawalls constructed on the land. Further efforts have been made by Tamada et al. (2015) to extend the applicability of IFORM to vertical or steep slope seawalls, and to the seawalls constructed at relatively deep water depth. In the previous studies, the model capability of overtopping prediction has been validated against the experiments by Tamada et al. (2002) and extracted CLASH database (Mase et al. 2013, 2016; Tamada et al., 2015). The results demonstrated that the overall prediction capability of IFORM is as good as other existing models such as Reis et al. (2008), Goda (2009b), and Van der Meer and Bruce (2014) and that the model is able to quickly provide consistent and useful information on wave runup and overtopping without detailed numerical computations. Under the conditions in which the relative freeboard is high and close to the threshold of overtopping occurrence, on the other hand, it has been observed that the model tends to underestimate the overtopping discharge compared with experimental observations (Mase et al. 2013, 2016; Tamada et al., 2015).

Since the tendency of underestimation is observed only for specific conditions of small overtopping discharge, it is considered that the reconstruction of the formula relating the runup and overtopping in broader conditions leads to more accurate estimation. In this study, accordingly, we attempt to re-calibrate the overtopping formula used in IFORM (Mase et al., 2013; Tamada et al., 2015). To provide reliable predictions under a broader range of overtopping conditions, a set of piecewise formulas is newly derived and implemented in the model. The accuracy of the original and refined model is verified against existing hydraulic experiments for inclined and vertical seawalls. The comparison with the predictions by representative existing overtopping models is also provided.

This paper is organized as follows: Section 2 explains the methodology adopted in the model refinement. Section 3 describes the method of model-performance assessment as well as the experimental datasets and representative existing models employed for comparison. The refinement of the original IFORM by Mase et al. (2013) is conducted in Section 4. Section 5 examines the results of the model-performance assessment by comparison with the existing experimental datasets and models. Additional discussion on the scaling and the modeling strategy of the overtopping discharge as well as the model uncertainty are provided in Section 6. Finally, the main outcomes are summarized in Section 7. The symbols used in the present paper are defined when first used.

2. Method of model refinement

2.1. Overview of Integrated Formula of wave overtopping and Runup Modeling

Mase et al. (2013) have developed an integrated prediction model for wave runup and overtopping for seawalls with smooth and impermeable surfaces that were named later as IFORM. In the model, non-dimensional overtopping discharge (q^*) is defined by

$$q^* = \frac{q}{\sqrt{gH_o'^3}} \tag{1}$$

where H_o' is the equivalent deep-water wave height (Goda, 2004, 2009b) and g represents the gravitational acceleration. Hereafter the subscript 'o' stands for the values at offshore boundary located in deep water. Deep-water wave characteristics are employed in the modeling to enable the prediction formula to be easily applicable for seawalls even constructed on the land.

IFORM is established based on a scheme that links wave runup and overtopping, because these two processes are closely related. Non-dimensional overtopping discharge is estimated based on predicted maximum runup (R_{max}), freeboard (R_c), and equivalent deep-water wave height as follows:

$$q^* = C\left[\Gamma\left(\frac{R_{max}}{H_o'}\right)^{\frac{3}{2}}\left\{1-\left(\frac{R_c}{H_o'}\right)\Big/\left(\frac{R_{max}}{H_o'}\right)\right\}^{\Omega}\right] \quad (\text{for } 0 \le R_c \le R_{max}) \tag{2a}$$

$$q^* = 0 \ (\text{for } R_{max} \le R_c) \tag{2b}$$

Equation (2a) includes three non-dimensional coefficients, C, Γ and Ω. The treatment of these empirical coefficients will be mentioned later.

Mase et al. (2013) and Tamada et al. (2015) validated that the model indicates high performance under the condition $h_t/H_o' < 3.0$ and $\tan\theta > 1/100$ where h_t is the water depth at the toe of the structure and $\tan\theta$ represents the bottom slope.

The maximum runup is estimated from the following equation where $R_{2\%}$ is the runup level exceeded by 2% of incident waves as

$$(R_{max})_{99\%,100} = 1.54R_{2\%} \tag{3}$$

In Eq. (3), $(R_{max})_{99\%,\ 100}$ means the runup height not exceeded in 99% of cases in runs of 100 incident waves. The 2% runup height is evaluated based on the following equations.

$$R_{2\%}/H_o' = 2.99 - 2.73\exp\left(-0.57\tan\beta/\sqrt{H_o'/L_o}\right) \tag{4}$$

in which L_o is the deep-water wavelength. A small safety margin is incorporated in the determination of the coefficients in the above formula. In Eq. (4), an imaginary slope, $\tan\beta$, is introduced to account for realistic compound profiles of actual sea bottom and seawall based on the method proposed by Nakamura et al. (1972) as

$$\tan\beta = \frac{(h_b + R_{2\%})^2}{2A} \tag{5}$$

in which A is the cross-sectional area between the breaking point (h_b: breaker depth) and the maximum wave runup level (Fig. 1). The computations of Eqs. (4) and (5) are conducted as an iterative procedure, in which the iteration was repeated until the relative difference between two consecutive estimations is smaller than 0.1%.

The breaker depth h_b for general beach profiles can be estimated by the random wave transformation model by Mase and Kirby (1993) with and without energy dissipation term by wave breaking. In particular, for planar beaches with bed slope of $\tan\theta$, the following formulas (Mase et al., 2016) that are fitted for the systematic computational results can be adopted.

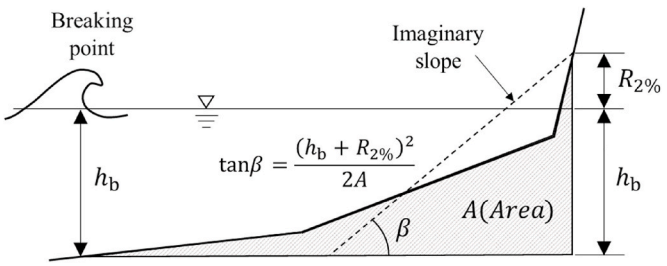

Fig. 1. Imaginary slope used in IFORM (according to Nakamura et al., 1972).

$$\frac{h_b}{H_o'} = a_0 + a_1 \exp\left[-\left(\frac{\ln\{(H_o'/L_o)/a_2\}}{a_3} \right)^2 \right] \tag{6}$$

$$a_0 = 30.2470 - 27.3440\exp\left[-\left\{ \frac{\ln(22.9130\tan\theta)}{5.4509} \right\}^2 \right] \tag{7a}$$

$$a_1 = -9.9467 + 8.9213\exp\left[-\left\{ \frac{\ln(29.3880\tan\theta)}{3.1264} \right\}^2 \right] \tag{7b}$$

$$a_2 = 0.0302 - 0.0023\exp\left[-\left\{ \frac{\ln(25.9160\tan\theta)}{1.7065} \right\}^2 \right] \tag{7c}$$

$$a_3 = 6.1291 - 3.5001\exp\left[-\left\{ \frac{\ln(36.3660\tan\theta)}{1.3457} \right\}^2 \right] \tag{7d}$$

These formulas are applicable as an approximation to the curved beaches and bar/trough beaches with representative slope tan θ over the nearshore covering the expected surf zone and its seaward portion. The breaker-depth model shown above is applicable in the range $0.002 < H_o'/L_o < 0.07$ and $1/100 < \tan\theta < 1/10$.

The coefficient C in Eq. (2a) was introduced by Tamada et al. (2015). It is determined by the following equations depending on the seawall slope (cot α). The condition denoted by cot $\alpha = 0$ corresponds to a vertical seawall.

$$C = 1 \ (\text{for } \cot\alpha \geq 2) \tag{8a}$$

$$C = 0.25\cot\alpha + 0.5 \ (\text{for } 0 \leq \cot\alpha < 2) \tag{8b}$$

If the gradient of seawall slope is gentler than 1/2, $C = 1$ is assigned; the formula on runup and overtopping discharge is then the same as those in Mase et al. (2013). If the slope of a seawall is steeper than 1/2 (e.g., vertical seawalls or 1:1 gradient seawalls), the runup height is computed from the following procedure. First $R_{2\%}$ is evaluated by Eq. (4) as for 1:2 gradient seawalls. Next, the maximum runup R_{max} is computed from Eq. (3). The overtopping discharge is then evaluated from Eq. (2) by multiplying the coefficient C that is determined by Eqs. (8a) and (8b) based on the actual slope of the seawall.

In Mase et al. (2013) and Tamada et al. (2015), the other two empirical coefficients in Eq. (2a) are set constant as follows.

$$\Gamma = e^{-4.000} \cong 0.018 \tag{9a}$$

$$\Omega = 6.240 \tag{9b}$$

The determination of these two coefficients will be re-examined and optimized later in the proceeding sections. A set of predictive equations together with the empirical coefficients of Eqs. (9a) and (9b) is hereafter called as the original IFORM for the sake of convenience.

The influence factors related to oblique attack as well as a berm, roughness elements on a slope, and the presence of a vertical wall on the top of a dike are not treated in Mase et al. (2013) and Tamada et al. (2015), and neither considered in the present study.

2.2. Re-evaluation of coefficients in overtopping formula suitable for a broader range of runup conditions

In IFORM, the overtopping discharge is estimated from maximum runup. The model is constructed based on the concept of Hedges and Reis model (Hedges and Reis, 1998; hereafter referred to as HR model, Fig. 2) that is described as follows:

$$q_{HR}^* = \Gamma\left(1 - R_{HR}^*\right)^{\Omega} \text{ for } R_{max} > R_c \tag{10a}$$

$$q_{HR}^* = 0 \text{ for } R_{max} \leq R_c \tag{10b}$$

$$q_{HR}^* = \frac{q}{\sqrt{gR_{max}^3}}, \quad R_{HR}^* = \frac{R_c}{R_{max}} \tag{11}$$

where q_{HR}^* stands for the normalized overtopping discharge and R_{HR}^* refers to the ratio of the freeboard of the seawall to the maximum runup level. It is noted that the normalization used in HR model in Eq. (11) and IFORM in Eq. (1) is different. This is because the normalization with equivalent deep-water wave height is more convenient for practical use. In IFORM, $(R_{max}/H_o')^{3/2}$ has thus been introduced in Eq. (2a) to exchange the overtopping discharge based on different definitions of normalization. This point will be further discussed in a later section. The HR model satisfies the following physical requirements: (i) wave overtopping does not occur when the maximum runup is lower than the freeboard of seawall, and (ii) overtopping discharge remains finite when the freeboard is zero. The two coefficients Γ and Ω in Eq. (10a) correspond to those in Eq. (2a) in IFORM. The Γ determines the overtopping discharge when R_{HR}^* is zero. The Ω governs the curvature of the curve in Fig. 2 that controls the relation between q_{HR}^* and R_{HR}^*.

In the original IFORM, the two coefficients Γ and Ω have been determined through the following procedure based on the experimental datasets for seawalls installed near the shoreline (Tamada et al., 2002) as shown in Fig. 3. First, the non-dimensional quantities X and Y are defined as:

$$X = \ln\left(1 - R_{HR}^*\right) \tag{12a}$$

$$Y = \ln\left(q_{HR}^*\right) \tag{12b}$$

The corresponding experimental results are plotted in Fig. 3. The plots indicate substantial scatter induced by the stochastic nature of wave overtopping. This kind of uncertainty may lead to substantial differences in the regression scheme utilized in prediction models. In the original IFORM, the focus was placed on the cases where the overtopping discharge is relatively large (approximately $X > -1$ in the figure), and the regression line was determined so that it could provide a conservative estimate of discharge rate for design (assessment) purposes. The relation between them has then been described by the line given by Eq. (13) as shown in Fig. 3.

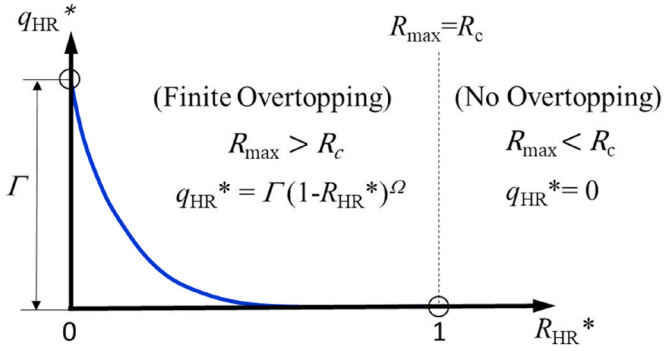

Fig. 2. Concept of Hedges and Reis (1998) model.

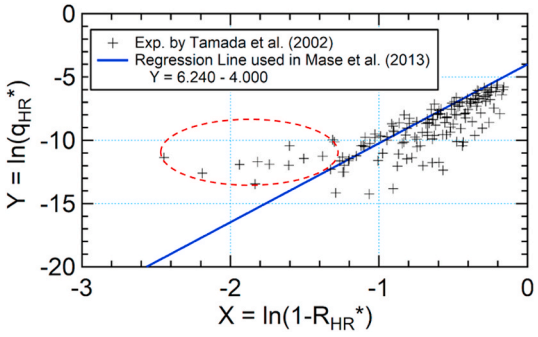

Fig. 3. Regression line used in the determination of Γ and Ω in the original IFORM.

$$Y = 6.240X - 4.000 \tag{13}$$

It is noted here that the underlying modeling concept in IFORM is similar to the 'design approach' in EurOtop (2018) rather than the 'mean value approach'.

Next, Γ and Ω were determined by Eq. (9a) and by Eq. (9b), respectively, as the Y-intercept and the slope of the regression line described by Eq. (13). In this way, the overtopping formula was established based on a single straight line over the whole area in Mase et al. (2013). In the area of relatively large X where R^*_{HR} is low and the overtopping discharge is high, Fig. 3 demonstrates that the adopted regression line passes through the area close to the upper limit of the scattered data and could provide safety prediction for design purposes. In contrast, the regression line is located far below the measured data in the area surrounded by a red ellipse in the figure. This implies that the model prediction tends to substantially underestimate the experimental observations in the range of small X (R^*_{HR} is close to unity).

In summary, the overtopping prediction by the original IFORM is in good agreement with experimental observations under the conditions of relatively large overtopping discharge, while the model tends to underestimate the overtopping discharge under the conditions of relatively small runup close to the threshold of overtopping occurrence. This tendency has been observed in the range of approximately $q^* < 10^{-4}$ in the previous studies (Mase et al., 2013; Tamada et al., 2015).

In this study, accordingly, an attempt has been made to optimize the prediction formula for overtopping discharge to achieve a high performance of the model prediction for a broader range of R^*_{HR}. The regression formula between the overtopping discharge and the runup is re-examined for further adjustment. The formulation has been reconstructed as a set of piecewise formulas for three ranges of X (or R^*_{HR}) so that it retains the high performance of the original IFORM in the range of relatively high value of X, while the tendency of underestimation in the range of small X is improved selectively.

3. Method of model-performance assessment

The performance of the original and refined model is examined by comparison with existing hydraulic experiments and well-known prediction models for inclined and vertical seawalls. The experimental datasets and existing models employed for comparison, the treatment of wave properties at deep-water, and the method of statistical evaluation are briefly described in the following.

3.1. Datasets employed for the assessment of model performance

3.1.1. Experimental datasets by Tamada et al. (2002) for inclined seawall

First of all, the applicability of the original and refined IFORM is validated by comparison with the measurements by Tamada et al. (2002) for inclined seawalls. Note that this dataset has been used as the basis of the development of IFORM. Table 1 lists the experimental conditions in the datasets consisting of the extracted data number and the range of main hydraulic and geometric parameters. Data of zero overtopping discharges were not used in the present analysis. The experiments were conducted in a wave flume of 25 m long, 0.5 m wide and 0.6 m high. For the generation of random waves, the Bretschneider-Mitsuyasu spectrum was used. The seawalls were installed at relatively shallow water or on land. More detailed information can be found in Mase et al. (2013).

Table 1
Experimental conditions in the experiments by Tamada et al. (2002).

Condition	Value
Number of data	150
Sea bottom slope tan θ	1/10, 1/30
Seawall front slope tan α	1/3, 1/5, 1/7
Deepwater significant wave steepness H_o/L_o	0.017, 0.036
Dimensionless seawall freeboad R_c/H_o	0.5~1.5
Dimensionless water depth at the toe of the seawall h_t/H_o	−0.27~0.50

3.1.2. Experimental datasets by Altomare et al. (2016) for inclined seawall

The applicability of the original and refined IFORM for inclined seawalls is then further examined through the comparison with experimental results that were conducted independently by other facilities. For this purpose, the experimental datasets of Altomare et al. (2016) have been used. The experiments were conducted at Flanders Hydraulics Research (FHR) in Belgium. The experimental data consists of two datasets (DS13-116 and DS13-168) that include 132 cases in total. Table 2 lists the experimental conditions in the extracted datasets consisting of the dataset name, the number of extracted data from each dataset and the range of the main hydraulic and geometric parameters. The seawalls were installed at relatively shallow water or on land. The details of the experiments at FHR can be found in Altomare et al. (2017) and Chen et al. (2015).

3.1.3. Experimental datasets extracted from CLASH database for vertical seawall

Next, the applicability of the original and refined IFORM is validated by comparison with the measurements for vertical seawalls extracted from the CLASH datasets. The data extraction was made for the cases of a plain vertical wall with smooth and impermeable surfaces that satisfy the conditions of $h_t/H_o' < 3.0$ and $\tan\theta > 0.01$. The data with RF (Reliable Factor) = 4 were considered to be unreliable and excluded from the analysis. The comparison was limited to the cases of simple cross-sections and the data with CF (Complexity Factor) > 1 were also excluded. Data of zero overtopping discharges were not used in the present analysis. Extraction resulted in 270 cases from 5 datasets. Table 3 lists the experimental conditions in each dataset consisting of the dataset name, the number of extracted data from each dataset, the range of the main hydraulic and geometric parameters.

Table 2
Experimental conditions of the datasets selected from the experiments by Altomare et al. (2016).

Dataset Id.	13–116	13–168	Total
Number of data	90	42	132
Sea bottom slope tan θ	1/35	1/50	1/35, 1/50
Seawall front slope tan α	1/3, 1/6	1/2	1/2, 1/3, 1/6
Deepwater significant wave steepness H_o/L_o	0.012~0.043	0.005~0.015	0.005~0.043
Dimensionless seawall freeboad R_c/H_o	0.38~0.78	0.26~2.55	0.26~2.55
Dimensionless water depth at the toe of the seawall h_t/H_o	−0.05~0.20	0.00~0.86	−0.05~0.86

Table 3
Experimental conditions in the extracted CLASH datasets.

Dataset Id.	DS-028	DS-224	DS-225	DS-502	DS-802	Total
Number of data	88	33	15	43	91	270
Sea bottom slope tan θ	1/10, 1/30	1/50	1/20	1/10, 1/50	1/10, 1/30	1/10, 1/20, 1/30, 1/50
Cotangent of seawall front slope cot α	0	0	0	0	0	0
Deepwater significant wave steepness H_o/L_o	0.014~0.041	0.009~0.044	0.018~0.041	0.015~0.063	0.004~0.033	0.004~0.063
Dimensionless seawall freeboad R_c/H_o	0.46~2.07	1.35~2.23	1.34~2.33	0.76~2.31	0.44~2.12	0.44~2.33
Dimensionless water depth at the toe of the seawall h_t/H_o	0.49~2.97	1.01~2.94	1.01~2.90	0.81~2.82	0.61~2.94	0.49~2.97

3.2. Existing overtopping models employed for the assessment of model performance

3.2.1. Prediction models for inclined seawall

For inclined seawalls, additional comparisons are conducted against the formulas by Altomare et al. (2016) and by Goda (2009b) among the existing overtopping prediction formulas. Hereafter these formulas are called the Altomare and Goda models, respectively. The Altomare model (adopted in EurOtop, 2018) has improved the applicable range of the model of Van Gent (1999) (adopted in EurOtop, 2007) by incorporating an equivalent (i.e. imaginary) slope that uses the wave height at the toe of the structure and $R_{2\%}$. The Altomare model has been tuned against the latest EurOtop datasets that include the two datasets (13–116 and 13–168) used in this study. The Goda model has been derived through the analysis of the datasets selected from the CLASH datasets. Wave properties at the toe of the structure are used for prediction in these models.

3.2.2. Prediction models for vertical seawall

For vertical seawalls, further comparisons were made with the existing overtopping models proposed by EurOtop (2018) and by Goda (2009b). It is noted that the EurOtop model is based on the EurOtop database including the CLASH datasets. The Goda model is also established based on the CLASH datasets. Wave properties at the toe of the structure are used for prediction in these models.

3.3. Treatment of wave properties at deep-water

Specification of the deep-water wave period is needed in the evaluation of deep-water wavelength in Eq. (4). In IFORM, the significant wave period $T_{1/3,o}$ is usually used for this purpose. The deep-water wave properties are specified as follows in the course of IFORM prediction

$$H_o^{'} = H_{1/3,o}\ ,\ T_o = T_{1/3,o}\ ,\ L_o = \frac{g}{2\pi}T_o^2 \tag{14}$$

in which $H_{1/3,o}$ and $T_{1/3,o}$ refers to the significant wave height and period, respectively, defined at the offshore (deep-water) boundary.

In the datasets of Altomare et al. and the extracted CLASH datasets, the information on the deep-water wave properties are given as the $H_{m0,o}$ (significant wave height computed from the spectrum), $T_{p,o}$ (peak wave period), $T_{m,o}$ (average wave period), and $T_{m\text{-}1,0,o}$ (spectral wave period). In EurOtop (2018), typical relations are described among the wave properties based on the different definitions as follows:

$$T_{1/3} \cong 1.1 \sim 1.25T_m \cong T_p \cong 1.1T_{m-1,0} \text{ and } H_{1/3} \cong H_{m0} \tag{15}$$

Goda (2009a) suggested slightly different relations

$$T_{1/3} \cong T_{m-1,0} \text{ and } H_{1/3} \cong 0.95H_{m0} \tag{16}$$

Referring to the description in EurOtop (2018) (Eq. (15)), the deep-water wave properties in IFORM are calculated as follows in this study for the datasets of Altomare et al. and CLASH.

$$T_o = T_{1/3,o} \cong 1.1T_{m-1,0,o} \text{ and } H_o^{'} = H_{1/3,o} \cong H_{m0,o} \tag{17}$$

It was confirmed that if the significant wave period $T_{1/3,o}$ is estimated based on $T_{p,o}$ or $T_{m,o}$ with the relation presented in Eq. (15), mostly similar results were obtained.

It is noted that the non-dimensional overtopping discharge is evaluated based on the wave characteristics at deep-water in IFORM, while it is evaluated based on the wave height at the toe of the structure in the formulas of the Altomare, Goda, and EurOtop models. For consistent comparison, when we apply the formulas in these models, the dimensional discharge rates are first computed by their formulas and then normalized by using the wave height at deep water as in IFORM.

3.4. Indices for statistical assessment of model performance

Goda (2009b) proposed the use of the geometric mean μ_{GM} and the geometric standard deviation σ_{GM} to evaluate the overall performance of the models

$$\mu_{GM} = \exp\left[\frac{1}{N}\sum_{i=1}^{N}\ln(r_i)\right] \tag{18}$$

Here, r_i is the ratio of predicted overtopping discharge to measured one (hereafter called as the ratio of overtopping prediction).

$$r_i = \frac{q_{\text{pred},i}}{q_{\text{meas},i}} \tag{19}$$

in which the subscripts "pred" and "meas" represent the results obtained from model prediction and experimental measurement, respectively. The scatter of data is evaluated with the geometric standard deviation σ_{GM} defined below:

$$\sigma_{GM} = \exp\left\{\left[\frac{1}{N}\sum_{i=1}^{N}\left((\ln(r_i))^2 - (\ln(\mu_{GM}))^2\right)\right]^{0.5}\right\} \tag{20}$$

In the mean value approach, the prediction model is usually calibrated so that μ_{GM} approaches unity. At the same time, however, 50% of prediction is considered to be below the measurement when $\mu_{GM} = 1$. For design purposes, accordingly, a parameter setting reproducing $\mu_{GM} = 1$ is not necessarily the best choice. Additional indices should be taken into account to assess the model performance. For this purpose, the five percent non-exceedance and exceedance values, or equivalently, the 90% confidence interval is often used. If the overtopping prediction ratio r_i is assumed to follow the log-normal distribution, 90% of the predicted ratio is to be located in the range between the five percent non-exceedance and exceedance values, $r_{L5\%}$ and $r_{U5\%}$, respectively.

$$r_{L5\%} = \frac{\mu_{GM}}{1.64\sigma_{GM}},\ r_{U5\%} = \mu_{GM} * 1.64\sigma_{GM} \tag{21}$$

These indices are also used in the assessment of the prediction performance when appropriate. The assumption of log-normal distribution is adopted also in many of the recent overtopping studies (e.g., Goda, 2009b; EurOtop, 2018; Liu et al., 2020). The validity of this assumption is examined later.

In Altomare et al. (2016) and EurOtop (2018), the overtopping formula has been presented based on 'mean value approach' and 'design (or assessment) approach'. The mean value approach estimates the mean value of the stochastic overtopping data. The design approach

incorporates some safety factor and can be used straightforwardly in the design procedures of coastal structures. Since the formulation of IFORM is close to the 'design approach', the comparison with EurOtop prediction is mainly made for the design approach. It is noted that the Goda model is considered to be categorized as the mean value approach.

4. Refinement of integrated runup-overtopping model

To obtain overtopping formulas that are applicable to a wide range of overtopping conditions, the model equations are empirically re-established as a set of piecewise formulas for the following three ranges of X:

(Zone-I) $-0.5 \leq X$

(Zone-II) $-1.4 < X < -0.5$

(Zone-III) $X \leq -1.4$

The zoning above was determined empirically through try and error basis. Conditions $X = -1.4$ and -0.5 correspond to $R_{max}/R_c = 1.33$ and 2.54, respectively.

Fig. 4 indicates that due to the scattering of observed data, the magnitude of overtopping discharge (corresponding to Y) substantially varies for the same value of normalized runup (corresponding to X). For design purposes, accordingly, the regression formulas were determined so that the line (curve) passes close to the upper limit of the scattered data. This kind of conservative determination of regression formulas implies that the prediction scheme adopted in the refined IFORM has some safety factor and the overall model predictions are expected to be larger than the mean of the scattered measurement data.

Zone-I corresponds to the case where the crest freeboard is relatively low (in other words, runup height is sufficiently high) and the resulting overtopping discharge becomes large. In this zone, it has been verified that the original IFORM provides satisfactory predictions of overtopping discharge (Mase et al., 2013; Tamada et al., 2015). And therefore, the same form is retained in this zone.

$$Y = 6.24X - 4.00 \quad (-0.5 \leq X) \tag{22}$$

As was mentioned before, the parameters Γ and Ω in Eq. (2) are determined from the slope and intercept of the regression line as

$$\Gamma = e^{-4.000} \cong 0.018 \ (-0.5 \leq X) \tag{23a}$$

$$\Omega = 6.240 \ (-0.5 \leq X) \tag{23b}$$

The overtopping formula in Zone-III was constructed as follows. In this zone, the variation of Y was quite gentle compared with other zones. Since the slope of the regression equation appears as a power index in Eq. (2a), it may have a significant influence on the estimation of overtopping discharge when the maximum runup height is close to

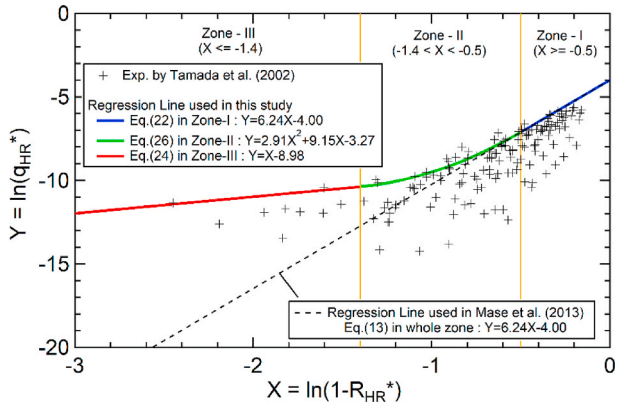

Fig. 4. Extension of the equation for discharge estimation.

overtopping threshold (*i.e.* $1-R_c/R_{max}$ is small). In the original IFORM, the use of Eq. (13) in this area resulted in the underestimation of overtopping discharge. In this study, accordingly, the slope of the regression line in Zone-III was set as unity because of the following two reasons. First, it represents the variation of Y in Zone-III quite well. And second, it is the minimum limit for the curve in the HR model (in Fig. 2) to be convex downward. The regression line was then set as shown below:

$$Y = X - 8.98 \ (X \leq -1.4) \tag{24}$$

The value of the intercept was determined empirically by trial and error approach. Based on the slope and intercept of the regression line given by Eq. (24), the two parameters Γ and Ω are determined as

$$\Gamma = e^{-8.98} \fallingdotseq 0.00013 \ (X \leq -1.4) \tag{25a}$$

$$\Omega = 1.000 \ (X \leq -1.4) \tag{25b}$$

Finally, the parabolic curve given by Eq. (26) was adopted in the central zone (Zone-II). The form of this curve was determined so that it can provide a smooth transition between the lines given by Eqs. (22) and (24) at both ends of the Zone-II.

$$Y = 2.91X^2 + 9.15X - 3.27 \ (-1.4 < X < -0.5) \tag{26}$$

In this zone, the values of Γ and Ω are determined from the slope B and the Y-intercept D of the tangential line to the parabolic curve. The values of B and D are not constant but vary with X as

$$B(X) = 5.82X + 9.15 \tag{27a}$$

$$D(X) = -3.27 - 2.91X^2 \tag{27b}$$

The values of Γ and Ω are then determined as functions of X as follows:

$$\Gamma = e^{D(X)} = e^{-3.27-2.91X^2} \ (-1.4 < X < -0.5) \tag{28a}$$

$$\Omega = B(X) = 5.82X + 9.15 \ (-1.4 < X < -0.5) \tag{28b}$$

In the course of the reconstruction of model equations, several other forms were tested. The form presented here has been adopted from the overall viewpoints of the consistency with the original IFORM, brevity of expressions, and overall prediction performance. Hereafter, the IFORM with the use of Eqs. (23), (25) and (28) is called as the refined IFORM.

5. Results of model-performance assessment

5.1. Comparison with the experiments by Tamada et al. (2002) for inclined seawall

The predictions of overtopping discharge by the original IFORM and refined IFORM are compared with experimental observations by Tamada et al. (2002) in a dimensionless form in Fig. 5. The data are classified into three groups according to the slope of the seabed. In the figures, three diagonal solid lines indicate the conditions that the prediction is 0.1 times, equal to, and 10 times the measured values. A 90% confidence interval is shown in the figure by dashed lines in blue where 5% of the data are estimated to fall below the interval and 5% above. A corresponding 50% exceedance level is indicated by the dash-dot line in red. Overall, the prediction by the original IFORM provides good agreement with the experiment in Fig. 5(a). The predicted values are mostly located slightly above the measurements, because a conservative determination was conducted for the coefficients during the formulation of IFORM. In the range where the normalized overtopping discharge is smaller than approximately 10^{-4}, however, the original IFORM tends to underestimate the overtopping discharge as mentioned before. In several cases, the underestimation of the overtopping discharge reached up to one or two orders of magnitude. In contrast, the accuracy of prediction in this zone is significantly improved in the refined IFORM in Fig. 5(b). Except

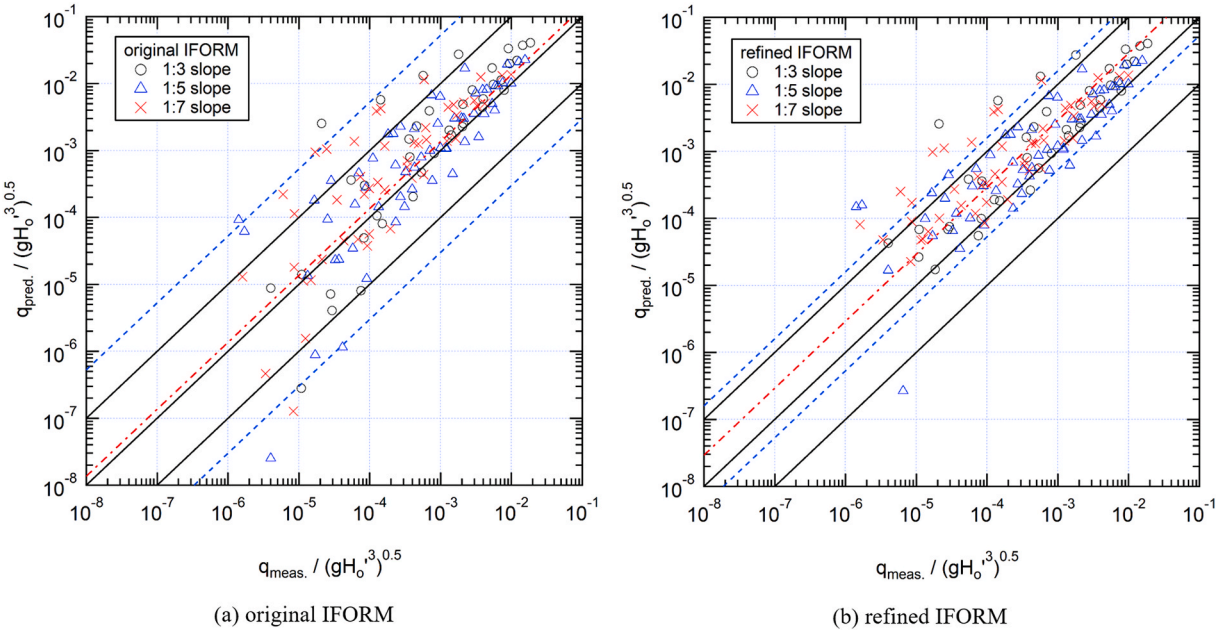

(a) original IFORM (b) refined IFORM

Fig. 5. Comparison of measurements and predictions: (a) original IFORM; (b) refined IFORM [Eqs. ((1), (2), (23), (25) and (28)].

for an outlier, all of the results are located in the range larger than 10^{-1} times of the measurements. In the area where the normalized overtopping discharge is larger, on the other hand, the refined IFORM provides the same estimations as to the original IFORM. It is noted that the prediction based on the refined IFORM provided a conservative estimate in the figure; namely, the predicted values are close to or larger than measured values. This is because Eqs. (22), (24) and (26) are determined so that they are located close to the upper limit of the scattered data. The characteristics of scattering in the plot are similar for different seabed slope.

The ratio of overtopping prediction is then plotted against the freeboard normalized by the maximum runup in Fig. 6. A 90% confidence interval is shown in the figure by dashed lines in blue, and 50% exceedance level is indicated by the dash-dot line in red. Since the original IFORM tends to underestimate the overtopping discharge in the range corresponding to Zone-III, the ratio of overtopping prediction obtained by the original IFORM exhibits a downward shift toward the right. These are significantly improved in the refined IFORM. Thus, it is confirmed that the prediction by the refined IFORM was selectively improved in Zones-II and –III. The new formulas successfully provide the conservative estimate of overtopping discharge for design purposes and indicate no shift over the whole range.

Both of the geometric mean (μ_{GM}) and geometric standard deviation (σ_{GM}) for the refined IFORM has been satisfactorily improved compared with the original one (Table 4). The use of the refined IFORM resulted in the μ_{GM} for overall data of 2.92 and the corresponding σ_{GM} is 3.34. If the ratio of overtopping prediction is assumed to follow the log-normal

Table 4
Comparison of model performance against Tamada's experiments.

tan(α)		1/3	1/5	1/7	Total
N		42	60	48	150
original IFORM	μ_{GM}	1.45	0.86	2.28	1.36
	σ_{GM}	7.33	84.55	4.76	23.70
	$r_{L5\%}$	0.12	0.01	0.29	0.03
	$r_{U5\%}$	17.43	119.25	17.80	52.86
Refined IFORM	μ_{GM}	2.76	2.26	4.22	2.92
	σ_{GM}	2.98	3.46	3.20	3.34
	$r_{L5\%}$	0.56	0.40	0.80	0.53
	$r_{U5\%}$	13.49	12.82	22.15	15.99

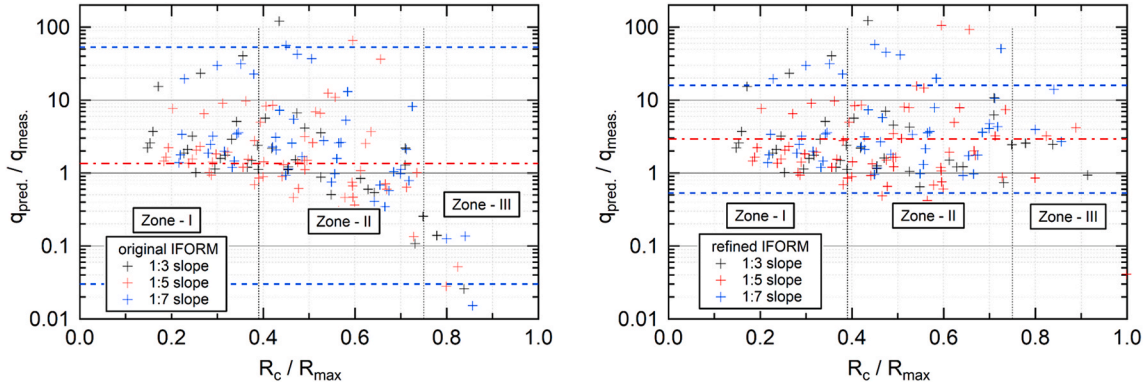

(a) original IFORM (b) refined IFORM

Fig. 6. Ratio of Overtopping prediction versus the crest freeboard normalized by maximum wave runup for the experiments by Tamada et al. (2002): (a) original IFORM; (b) refined IFORM [Eqs. ((1), (2), (23), (25) and (28)]. Separation of Zone-I, II, and III are indicated consistently as in Fig. 4.

distribution, 90% of the predicted data is to be located in the range between approximately 0.5 and 16 times the measured values.

Fig. 7 indicates the relation between the non-dimensional overtopping discharge and non-dimensional maximum runup height in the refined IFORM. The data are classified into five groups according to the ratio of the freeboard to deep-water wave height. The markers indicate the experimental results by Tamada et al. (2002). The curves in the figure are obtained by the refined IFORM. The curves represent the general trend of the measurement well. Compared with the original IFORM (e.g. Fig. 21 in Mase et al. (2013)), the curves are modified so that they envelop the measured results over the whole range of runup, especially where the non-dimensional discharge is small.

5.2. Comparison with the experiments by Altomare et al. (2016) for inclined seawall

Next, the original and refined IFORM were applied to the test conditions of the experiments by Altomare et al. (2016) listed in Table 2. The prediction of overtopping discharge by the original IFORM is compared with observations in a dimensionless form in Fig. 8(a). The data are classified into two groups according to datasets. In the figure, three diagonal solid lines indicate the conditions that the prediction is 0.1 times, equal to, and 10 times the measured values. A 90% confidence interval is shown in the figure by dashed lines in blue where 5% of the data are estimated to fall below the interval and 5% above. A corresponding 50% exceedance level is indicated by the dash-dot line in red. Qualitatively, the original IFORM reproduces the overall variation of overtopping discharge, and most of the predictions lie between the lines that indicate the prediction is 0.1 times and 10 times the measured values. However, it tends to underestimate the experimental observation. This tendency is more apparent for small values of overtopping discharge. For several cases in DS-13-168, in particular, the original IFORM underestimates the overtopping discharge up to one to three orders of magnitude. Comparisons between the refined IFORM predictions and measurements are demonstrated in Fig. 8(b). Besides, the ratio of overtopping prediction is plotted against the experimental non-dimensional discharge in Fig. 9. A 90% confidence interval is shown in the figures by dashed lines in blue where 5% of the data are estimated to fall below the interval and 5% above. A corresponding 50% exceedance level is indicated by the dash-dot line in red. Compared with the predictions by the original IFORM, the prediction accuracy is significantly improved by the refined IFORM. From the figures, it is clear that the tendency of underestimation is improved in the area of small

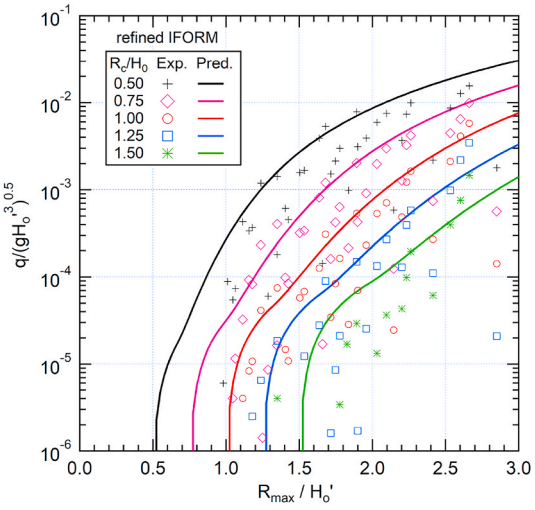

Fig. 7. Relation between non-dimensional maximum wave runup and non-dimensional wave overtopping. The solid lines are obtained by the refined IFORM. The markers indicate experimental results by Tamada et al. (2002).

overtopping. The prediction for the cases of outliers in Fig. 8(a) are significantly improved in Fig. 8(b). The width of the 90% confidence interval is substantially reduced and the estimations by the refined IFORM are concentrated closer to the line indicating that prediction and measurement are equal except for a few cases. The ratio of overtopping prediction is plotted against measured overtopping discharge in Fig. 9. The overall reproducibility is satisfactory. From a detailed inspection of the figure, a decreasing trend is captured for DS13-116, while an increasing trend is recognized for DS13-168. A similar tendency is observed in the prediction by the Altomare model described later in Fig. 11.

Both of the geometric mean (μ_{GM}) and geometric standard deviation (σ_{GM}) for the refined IFORM have been satisfactorily improved compared with the original IFORM (Table 5). The use of the refined IFORM resulted in the μ_{GM} for overall data of 0.77 and the corresponding σ_{GM} is 2.24. If the ratio of overtopping prediction is assumed to follow the log-normal distribution, 90% of the predicted data is to be located in the range between 0.21 and 2.81 times the measured values. The corresponding values for the original IFORM are 0.33 and 15.64 for μ_{GM} and σ_{GM}, respectively. The μ_{GM} and σ_{GM} values for each of the datasets are also listed in Table 5. It is found that the prediction performance of the refined IFORM has been improved for each of the datasets. A comparison of the results against the two datasets indicated that the μ_{GM} becomes smaller while σ_{GM} became larger in DS-168. This is commonly seen in both of the original and refined IFORM.

It is noted that although the IFORM has been modeled to provide a conservative prediction for design purposes, the estimation by the refined IFORM still slightly underestimates the measurements (the geometric mean is slightly smaller than unity) here. This point will be discussed in a later section.

The comparison between the prediction by existing models and the measurements are shown in Fig. 10. In the figures, three diagonal solid lines indicate the conditions that the prediction is 0.1 times, equal to, and 10 times the measured values. The ratio of overtopping prediction is plotted against the experimental non-dimensional discharge in Fig. 11. A 90% confidence interval is shown in the figures by dashed lines in blue where 5% of the data are estimated to fall below the interval and 5% above. A corresponding 50% exceedance level is indicated by the dash-dot line in red. The Altomare model provided quite satisfactory predictions. This is reasonable since the model has been tuned to the conditions including the datasets used in the present study. Most of the cases are located between 1 and 10 times the measured values. The values of μ_{GM} and σ_{GM} for the overall cases are 2.57 and 1.74, respectively, as shown in Table 5. If the ratio of overtopping prediction is assumed to follow the log-normal distribution, 90% of the predicted data is to be located in the range between 0.90 and 7.33 times the measured values. It is noted that in this figure the model prediction by the Altomare model is based on the coefficients proposed for the design approach. If the coefficients in the mean value approach are used, the plot will be more concentrated along the line indicating that prediction and measurement are equal. For the mean value approach, the corresponding μ_{GM} and σ_{GM} are 1.32 and 1.74, respectively. In contrast, the Goda model indicates significant scattering and drastic overestimation up to the order of 10^2 for substantial numbers of cases. The values of μ_{GM} and σ_{GM} for the overall cases are 14.25 and 7.32, respectively, as shown in Table 5. The μ_{GM} and σ_{GM} values became large for DS11-116.

Examination of Figs. 8–11 and Table 5 demonstrates that the quantitative reproducibility of the refined IFORM is close to that of the Altomare model. The overall performance is sufficiently high compared with the Goda model. Taking into account that the IFORM is developed independently without tuning to these datasets, the overall model performance is considered to be satisfactory.

5.3. Comparison with the extracted CLASH datasets for vertical seawall

Finally, the original and refined IFORM are applied to the test

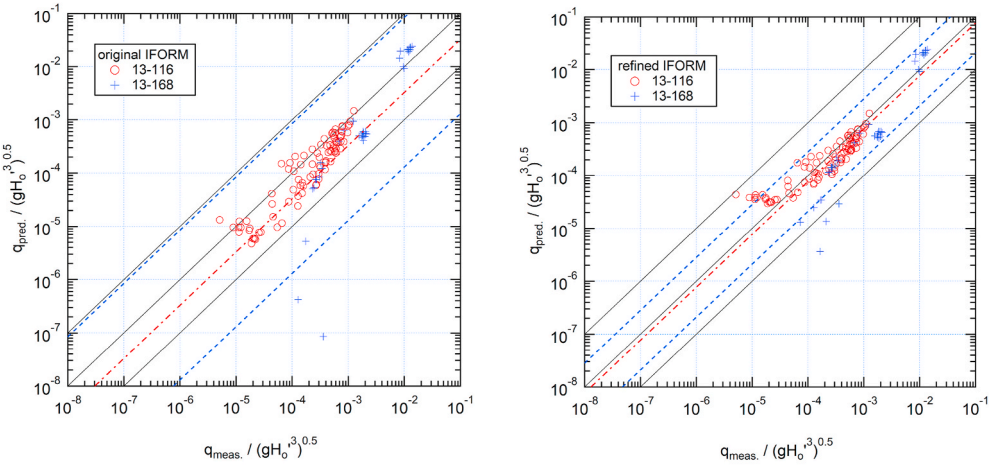

(a) original IFORM (b) refined IFORM

Fig. 8. Comparisons between measurements of Altomare et al. (2016) and model prediction: (a) original IFORM; (b) refined IFORM.

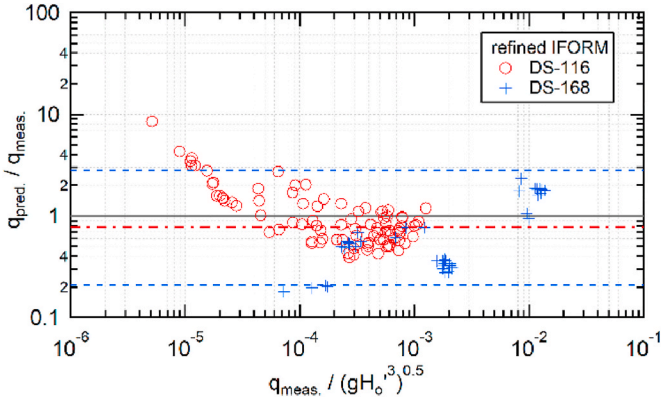

Fig. 9. Ratio of overtopping prediction versus the non-dimensional overtopping discharge obtained by the experiments by Altomare et al. (2016). The predicted values are based on the refined IFORM [Eqs. ((1), (2), (23), (25) and (28)].

Table 5
Comparisons of model performance against Altomare's experiments.

Dataset Id.		13–116	13–168	Total
N		90	42	132
original IFORM	μ_{GM}	0.58	0.10	0.33
	σ_{GM}	1.78	100.58	15.64
	$r_{L5\%}$	0.20	0.001	0.013
	$r_{U5\%}$	1.68	16.10	8.47
refined IFORM	μ_{GM}	0.94	0.49	0.77
	σ_{GM}	1.83	2.68	2.24
	$r_{L5\%}$	0.31	0.11	0.21
	$r_{U5\%}$	2.82	2.14	2.81
Goda (2009b)	μ_{GM}	20.63	6.45	14.25
	σ_{GM}	7.83	4.79	7.32
	$r_{L5\%}$	1.61	0.82	1.19
	$r_{U5\%}$	264.91	50.67	171.07
Altomare et al. (2016) (EurOtop (2018)) design approach	μ_{GM}	2.66	2.53	2.57
	σ_{GM}	1.80	1.72	1.74
	$r_{L5\%}$	0.90	0.90	0.90
	$r_{U5\%}$	7.85	7.14	7.33

conditions of the extracted CLASH dataset for plain vertical seawall listed in Table 3. The prediction of overtopping discharge by the original and refined IFORM are compared with the experimental observations in the dimensionless form in Fig. 12. The data are classified into five groups according to the dataset. In the figures, three diagonal solid lines indicate the conditions that the prediction is 0.1 times, equal to, and 10 times the measured values. A 90% confidence interval is shown in the figure by dashed lines in blue where 5% of the data are estimated to fall below the interval and 5% above. A 50% exceedance level is indicated by the dash-dot line in red. The original IFORM in Fig. 12(a) qualitatively reproduces the overall variation of overtopping discharge, and most of the predictions lie between the lines that indicate the prediction is 0.1 times and 10 times the measured values. However, for several cases located around $q^*_{meas.} = 10^{-4}$, the original IFORM underestimates the overtopping discharge up to one to three orders of magnitude. In Fig. 12(b), the predictions by the refined IFORM are improved. In particular the improvement in prediction for the cases of outliers in Fig. 12(a) is significant. The predictions by the refined IFORM are more closely concentrated slightly above the line indicating that prediction and measurement are equal. The ratio of overtopping prediction is plotted against the experimental non-dimensional discharge in Fig. 13. A 90% confidence interval is shown in the figure by dashed lines in blue where 5% of the data is estimated to fall below the interval and 5% above, and the corresponding 50% exceedance level is indicated by the dash-dot line in red. In the figure, the ratio of predicted to measured discharge is located above unity for most of the cases.

The μ_{GM} and σ_{GM} are listed in Table 6. Both of the geometric mean and standard deviation for the refined IFORM seems satisfactory. The use of the refined IFORM resulted in the μ_{GM} for overall data of 1.95 and the corresponding σ_{GM} is 2.57. Comparison with the original IFORM reveals that the scattering is improved: σ_{GM} varies from 3.93 by the original IFORM to 2.57 by the refined IFORM. The μ_{GM} value by the refined IFORM is more conservative than that by the original IFORM. If the ratio of overtopping prediction is assumed to follow the log-normal distribution, 90% of the data predicted by the refined IFORM is to be located in the range between 0.46 and 8.22 times the measured values. Some of the predictions corresponding to the cases of 1/50 slope (DS-224 and DS502) resulted in slight underestimation ($\mu_{GM} < 1$). This will be addressed later.

The comparison between the prediction by existing models and extracted CLASH datasets are shown in Figs. 14 and 15. In the figures, three diagonal solid lines indicate the conditions that the prediction is 0.1 times, equal to, and 10 times the measured values. A 90% confidence

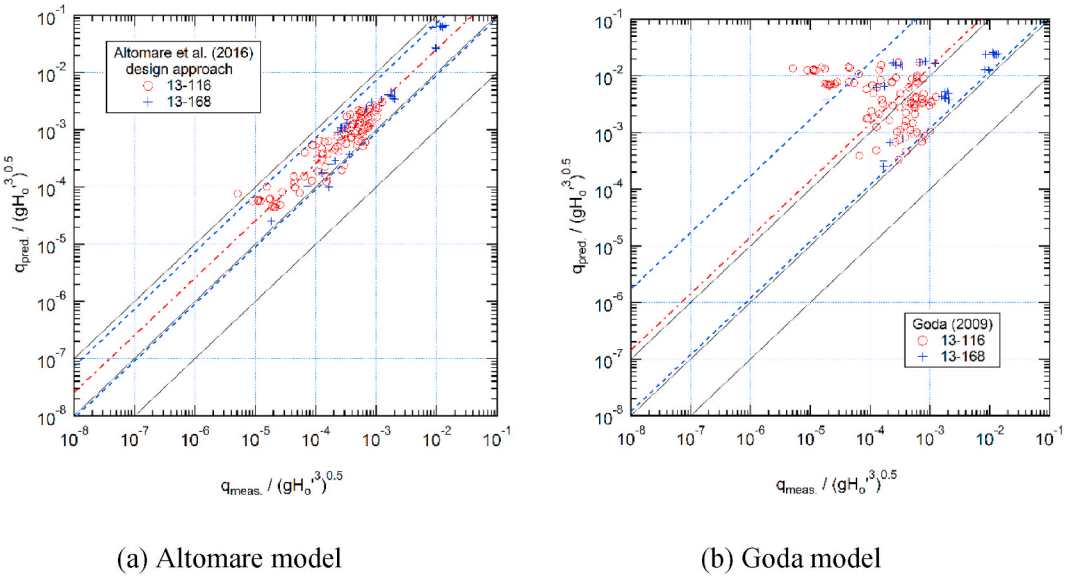

Fig. 10. Comparisons between measurements of Altomare et al. (2016) and model prediction: (a) Altomare model; (b) Goda model.

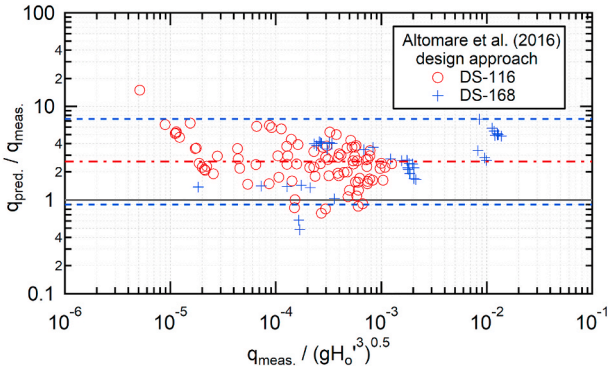

Fig. 11. Ratio of overtopping prediction versus the non-dimensional overtopping discharge obtained by the experiments by Altomare et al. (2016). The predicted values are based on the formulas by Altomare et al. (2016) with coefficients in the design approach.

interval is shown in the figure by dashed lines in blue where 5% of the data are estimated to fall below the interval and 5% above. A corresponding 50% exceedance level is indicated by the dash-dot line in red. It is noted that EurOtop (2018) model has been tuned for the EurOtop2018 database including the CLASH dataset. Also, the Goda model has been tuned for the CLASH dataset including the five sub-datasets in Table 3. EurOtop2018 model provides mostly satisfactory predictions. The values of μ_{GM} and σ_{GM} for the overall cases are 1.71 and 1.94, respectively (Table 6). It is noted that in this figure the model prediction by EurOtop2018 model is based on the coefficients proposed for the design approach. If the coefficients in the mean value approach are used, the plot will be more concentrated along the line indicating that prediction and measurement are equal. For the mean value approach, the corresponding μ_{GM} and σ_{GM} are 1.19, 1.93, respectively. The Goda model indicates satisfactory prediction except for a couple of cases. In total, the Goda model slightly underestimates the measurements. The values of μ_{GM} and σ_{GM} for the overall cases are 0.79 and 2.24, respectively. In Fig. 15, the ratios of overtopping predictions are plotted. The figures show that when $q^*_{meas.} < 10^{-4}$, both models indicate a common tendency of slight overestimation.

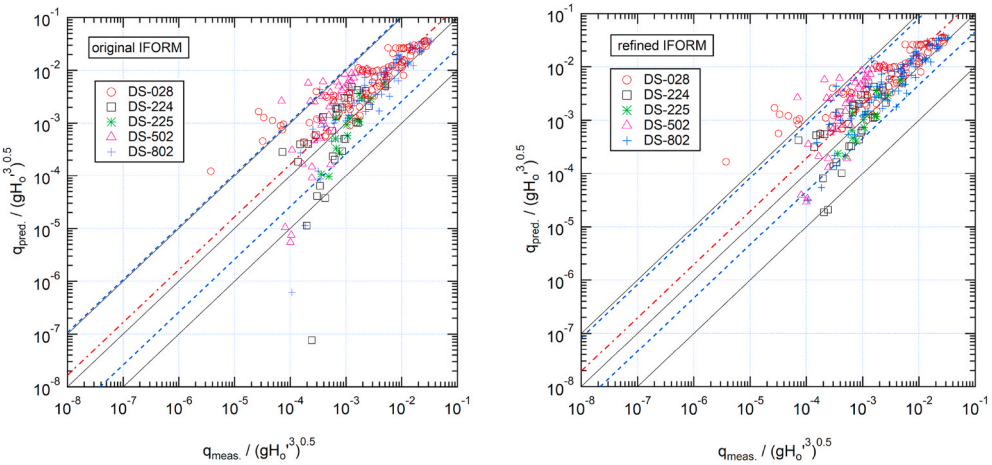

Fig. 12. Comparisons between extracted CLASH dataset and model prediction: (a) original IFORM; (b) refined IFORM [Eqs. ((1), (2), (23), (25) and (28)].

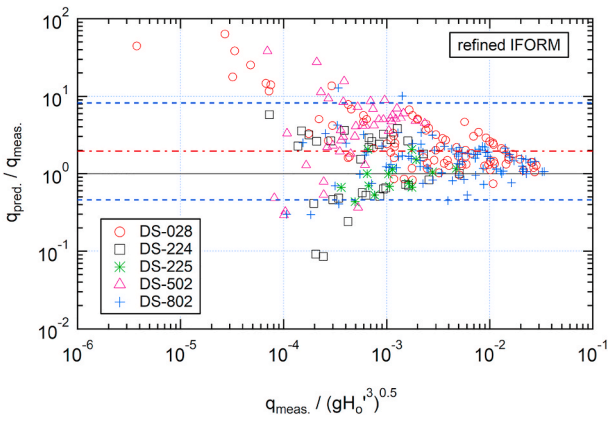

Fig. 13. Ratio of overtopping prediction versus the non-dimensional overtopping discharge in extracted CLASH dataset. The predicted values are based on the refined IFORM [Eqs. ((1), (2), (23), (25) and (28)].

Table 6
Comparisons of model performance against extracted CLASH datasets.

Dataset Id.		DS-028	DS-224	DS-225	DS-502	DS-802	Total
N		88	33	15	43	91	270
original IFORM	μ_{GM}	2.57	0.58	0.75	3.01	1.36	1.66
	σ_{GM}	2.46	11.82	1.92	3.96	2.38	3.93
	$r_{L5\%}$	0.64	0.03	0.24	0.46	0.35	0.26
	$r_{U5\%}$	10.38	11.26	2.36	19.56	5.30	10.70
refined IFORM	μ_{GM}	2.64	1.17	0.93	3.52	1.48	1.95
	σ_{GM}	2.51	2.89	1.56	2.94	1.79	2.57
	$r_{L5\%}$	0.64	0.25	0.36	0.73	0.51	0.46
	$r_{U5\%}$	10.85	5.55	2.37	16.96	4.34	8.22
Goda (2009b)	μ_{GM}	1.23	0.71	0.46	0.59	0.68	0.79
	σ_{GM}	2.41	2.14	1.43	2.43	1.68	2.24
	$r_{L5\%}$	0.31	0.20	0.20	0.15	0.25	0.22
	$r_{U5\%}$	4.86	2.49	1.08	2.35	1.87	2.90
EurOtop (2018)	μ_{GM}	2.15	1.76	1.03	1.40	1.63	1.71
design approach	σ_{GM}	2.42	1.51	1.29	1.62	1.64	1.94
	$r_{L5\%}$	0.54	0.71	0.49	0.53	0.61	0.54
	$r_{U5\%}$	8.53	4.36	2.18	3.72	4.38	5.44

It is noted again that the IFORM is developed without tuning to the CLASH datasets. Nevertheless, the overall comparisons of Figs. 12–15 and Table 6 clarify that the performance of the refined IFORM seems to be as good as the models developed based on the CLASH datasets. The refined IFORM can be applied in a wide range of conditions for vertical walls.

5.4. Overall examination of model performance and underlying assumption

The overall model performance is briefly summarized here. The geometric mean of the ratio of overtopping predictions against all of the datasets used in this study is $\mu_{GM,all} = 1.74$. Accordingly, the predictions based on the refined IFORM generally provide conservative estimations. The corresponding standard deviation is $\sigma_{GM,all} = 3.03$. If the ratio of overtopping prediction is assumed to follow the log-normal distribution, 90% of the data predicted by the refined IFORM is to be located in the range between 0.35 and 8.64 times the measured values.

To examine the validity of the assumption of log-normal distribution of r_i, the cumulative relative frequency of ln (r_i) is plotted in Fig. 16. The horizontal axis is normalized with its mean and standard deviation. The dashed lines in red represent the levels where 5, 50, and 95% of the data are located below in the actual prediction results. The corresponding plot for the theoretical standard normal distribution (mean = 0 and standard deviation = 1) is also plotted for reference. The dashed lines in blue represent the levels where 5, 50, and 95% of the data are located below in the theory. The overall agreements between the two curves are generally good and the correspondence of the 90% confidence intervals looks reasonable. These results thus validate the assumption of log-normal assumption of the ratio of overtopping prediction.

Moreover, the ratio of overtopping prediction for all of the datasets is plotted against the representative non-dimensional parameters in Fig. 17 (a) ~ (c). A 90% confidence interval under the assumption of log-normal distribution of r_i is shown in the figure by dashed lines in blue where 5% of the data are estimated to fall below the interval and 5% above. A corresponding 50% exceedance level is indicated by the dash-dot line in red. Fig. 17 (a) indicates that the scatter of the prediction ratio increases as the overtopping discharge becomes small. This is related to the difficulty in the accurate measurements of small overtopping volume. A small error in measurements (or also in predictions) results in a large scatter. Similar features are observed for the prediction by other representative models in the present study (Fig. 15) and other studies (e.g. Figs. 5, 13, 17 and 18 in Goda, 2009b). The prediction for the small overtopping discharge also has a tendency to be located above the overall mean. This tendency is common to the results by EurOtop and Goda models in Fig. 15. Fig. 17 (b) and (c) demonstrate that the ratio of overtopping prediction has no bias against the relative freeboard and wave steepness. As was mentioned before, the plots below the 5% level

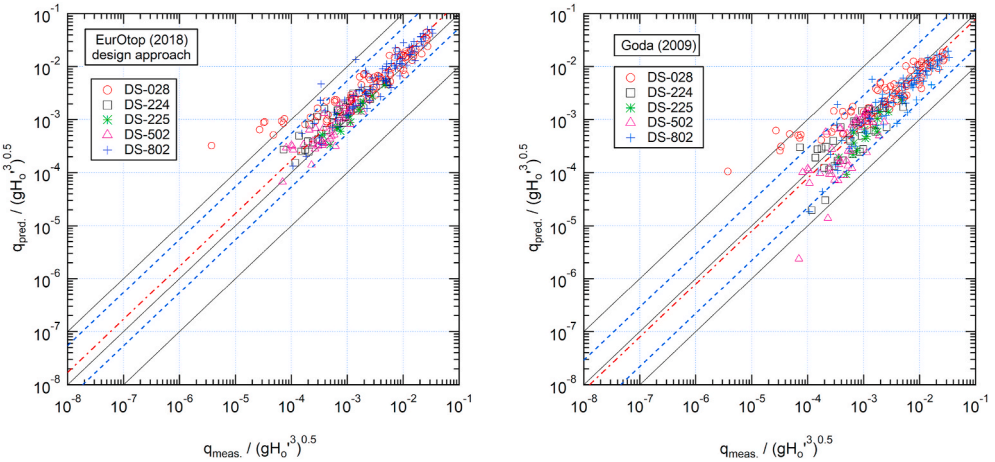

(a) EurOtop model (b) Goda model

Fig. 14. Comparisons between extracted CLASH dataset and model prediction: (a) EurOtop model with coefficients in the design approach; (b) Goda model.

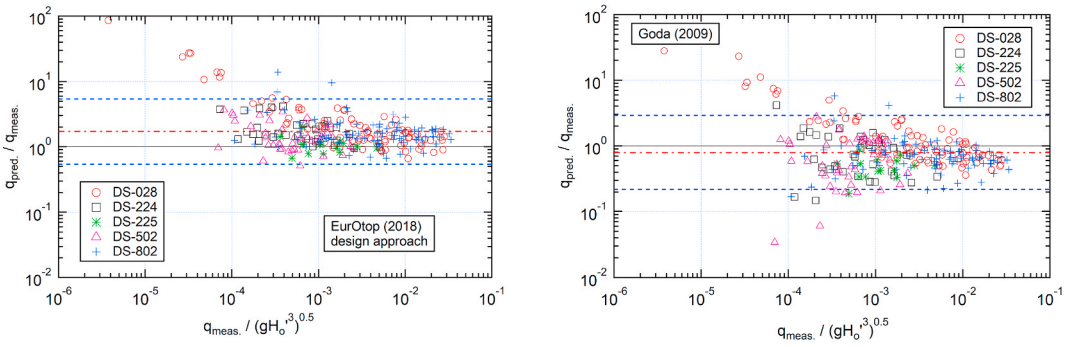

(a) EurOtop model (b) Goda model

Fig. 15. Ratio of overtopping prediction versus the non-dimensional overtopping discharge in extracted CLASH dataset: (a) EurOtop model with coefficients in the design approach; (b) Goda model.

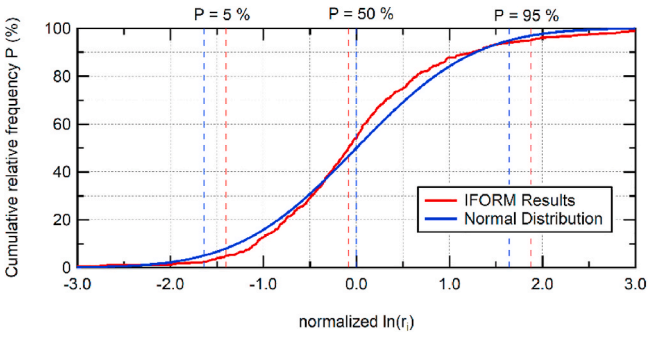

Fig. 16. Cumulative relative frequency of the logarithm of the ratio of overtopping prediction normalized with the mean and standard deviation. The predicted values are based on the refined IFORM [Eqs. ((1), (2), (23), (25) and (28)]. Prediction results for all of the datasets used in this study are included. The corresponding curve representing the standard normal distribution (mean = 0 and standard deviation = 1) is also plotted for reference.

in Fig. 17 (c) mainly belong to the cases of 1/50 slope. This will be discussed in the proceeding section.

6. Discussion

6.1. Scaling of overtopping discharge

Recently, Ibrahim and Baldock (2020) (hereafter referred to as IB2020) demonstrated that the overtopping volume can be properly expressed in terms of 'deficit in freeboard' defined as follows.

$$\delta = \frac{R_{max} - R_c}{R_{max}} = \left(1 - R^*_{HR}\right) = 1 - \frac{R_c}{R_{max}} \tag{29}$$

More recently, Altomare et al. (2020) further discussed the IB2020's scaling laws. They made a novel attempt to find a generalized model for mean wave overtopping discharge assessment of smooth and impermeable sea dikes. Differently from other approaches, an innovative genetic algorithm called Evolutionary Polynomial Regression (EPR) has been employed. EPR assisted the identification of the main explanatory variables governing the overtopping. Their results clarified that 1) the deficit in freeboard is a key explanatory variable for the wave overtopping assessment, and 2) the use of this parameter can reduce the scatter of experimental data. Furthermore, EPR proved that concepts such as imaginary slope or equivalent slope provide an accurate estimate of the processes that occur on the foreshore and dike and lead to wave transformation and breaking, finally affecting the overtopping phenomenon.

The two coefficients Γ and Ω in the refined IFORM are functions of deficit in freeboard because they are expressed in terms of $X = \ln(\delta)$. Hedges and Reis (1998) mentioned that the Γ and Ω parameters in the HR model may be influenced by the seaward profile of the structure. The expression adopted in the refined IFORM is more specific at this point. With the use of the deficit in freeboard, Eq. (2a) can be rewritten as

$$q^* = \frac{q}{\sqrt{gH_0'^3}} = C\left(\frac{R_{max}}{H_o'}\right)^{\frac{3}{2}}\left[\Gamma(\delta)\left\{1 - \frac{R_c}{R_{max}}\right\}^{\Omega(\delta)}\right] = \left(\frac{R_{max}}{H_o'}\right)^{\frac{3}{2}} C[\Gamma(\delta)\delta^{\Omega(\delta)}] \tag{30}$$

The quantities in the square bracket are expressed as a function of δ. Namely, the overtopping discharge in the refined IFORM is modeled in a form that is directly related to the deficit in freeboard.

Furthermore, if we adopt an alternative form of normalization (HR-type form) as in Eq. (11), Eq. (30) is rearranged as

$$q^*_{HR} = \frac{q}{\sqrt{gR_{max}^3}} = C[\Gamma(\delta)\delta^{\Omega(\delta)}] \tag{31}$$

If we consider gently-sloped seawalls, the coefficient $C = 1$ as in Eq. (8a). Then, in the prediction by the refined IFORM, the deficit in freeboard becomes the only governing parameter for the mean overtopping discharge normalized with the maximum runup. More in general, the similar consideration holds for the HR-type model. The successful application of the refined IFORM in the present study for a wide range of installation condition suggests that in the initial modeling process it is considered to be effective to scale the overtopping discharge with the runup height, in which the influence of not only the wave height, but also the wave period (wavelength) and others are incorporated. The consideration above is expected to hold for seawalls with steep slopes (for cases corresponding to Eq. (8b): $C < 1$). If the formulation given by Eq. (31) is valid for a wide range of conditions, further considerations are possible as shown in the following.

As previously mentioned, the normalization by H_o' is more preferable in practical situations. To adopt this form, the exchange between the different definitions of normalization becomes necessary. As a result, Eq. (30) indicates that the discharge normalized by H_o' is governed not only by δ but also by R_{max}/H_o' (appearing as an exchange ratio between different types of normalization). Namely, there appear two principal non-dimensional parameters. With these parameters, Eq. (30) is composed of the products of the following two components. The first component (C1) in front of the square brackets expresses to what extent the runup is amplified in relation to the incident wave height. The latter component (C2) in the square brackets regulates the overtopping volume q^*_{HR} for the given value of δ. Note that the estimation of R_{max} is related to both of the processes. Accordingly, the two fundamental

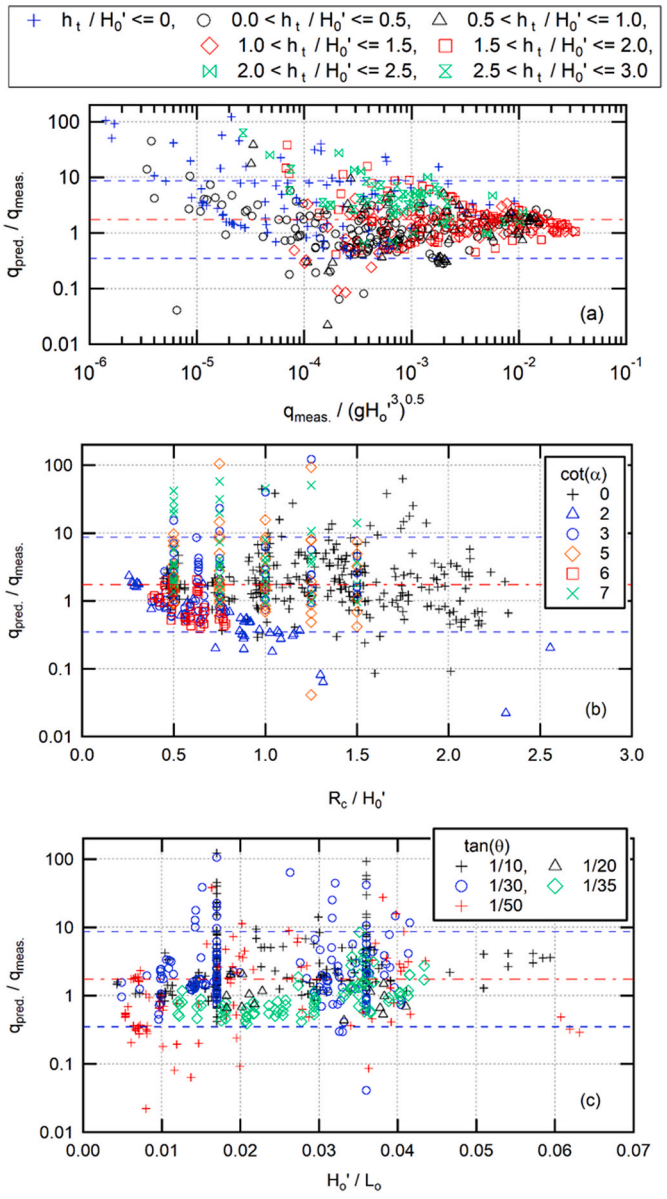

Fig. 17. Ratio of overtopping prediction versus the (a) non-dimensional overtopping discharge, (b) relative freeboard, and (c) wave steepness in all of the datasets used in this study. The predicted values are based on the refined IFORM [Eqs. ((1), (2), (23), (25) and (28)].

processes in the development of an overtopping model are recognized as (1) to establish an accurate runup model and (2) to formulate the relation between the runup and overtopping discharge in terms of the deficit in freeboard and the overtopping discharge scaled with the runup height. If each component is modeled properly, the prediction formula for overtopping discharge can then be obtained straightforwardly by the combination of them, in principle, as in IFORM or HR-type models. In the modeling of overtopping discharge, the following type of formulation has often been used (e.g., Goda (2009b), EurOtop (2007)).

$$\frac{q}{\sqrt{gH_{m0}^3}} = a\exp\left[-b\frac{R_c}{H_{m0}}\right] \tag{32}$$

Based on the analogy with the form in Eq. (30), it is deduced that the exponential term may correspond to the modeling of C2 and the coefficient a may represent the modeling of C1. The considerations above provide a new insight into the scaling and the modeling strategy of overtopping discharge.

Moreover, IB2020 introduced the volume of overtopping per wave as

$$V = qT_o \tag{33}$$

If we introduce the run-up scaling proposed by Hunt (1959) according to IB2020,

$$R_{max} \cong \sqrt{H_o' L_o} \tan\beta = \xi H_o' \tag{34}$$

in which ξ is the surf-similarity parameter,

$$\xi = \frac{\tan\beta}{\sqrt{H_o'/L_o}} \tag{35}$$

it can be shown that the overtopping volume per wave is scaled for the refined IFORM as

$$V = \sqrt{2\pi}\left(H_o' L_o \tan\beta\right)\sqrt{\xi}\, C\Gamma(\delta)\delta^{\Omega(\delta)} \tag{36}$$

The above form, which is derived from the refined IFORM (or, more generally, from the HR model), is consistent with the expression proposed by IB2020 (Eqs. (24) and (25) in their paper). The differences are that Eq. (36) explicitly include the surf-similarity parameter and that the expression for the δ-related part is more generalized. The form above may be useful as an alternative candidate for the scaling of the volume of overtopping per wave.

A brief discussion is given here on the power of tan β in the scaling of Eq. (36). In the scaling based on the refined IFORM, the power of the imaginary slope tan β becomes 3/2 in Eq. (36) because ξ includes $(\tan\beta)^{1/2}$. On the other hand, the power of beach slope is set as 1 or 1/2 in IB2020 (see Eqs. (24) and (25) in IB2020) and 1/2 in EurOtop (see Eq. (11) in IB2020). This is considered to be related to the difference in the definition of wave height. Namely, the representative wave height H represents $H_{1/3,o}$ at deep water in IFORM, while $H_{m0,-1,toe}$ after breaking in IB2020 and EurOtop. The $H_{m0,-1,toe}$ is influenced by the bottom slope through wave breaking. It is then logical to expect that the power of the beach slope takes different values for different definitions of representative wave height. The power should be discussed with the selection of the representative wave properties in the scaling formula. Moreover, the definition of beach slope itself is different depending on the model, and the influence of beach slope is also included in the estimation of the imaginary slope and deficit in freeboard.

Although the modeling strategy and selection of proper scaling of overtopping prediction deserves further investigation, it is beyond the scope of the present paper. More detailed examination on these issues are underway.

6.2. Uncertainty included in the model prediction

Since the refined IFORM has been modeled to provide a conservative prediction for design purposes, the model is expected to provide the value of geometric mean larger than unity. This is attained for most of the conditions in this study. Nevertheless, it is noted here that for certain datasets the estimations by the refined IFORM still slightly underestimated the measurements (the geometric mean was slightly smaller than unity). The underestimation was observed for the experiments of Altomare with 1/35 (DS13-116) and 1/50 (DS13-168) slope seabed and the cases of 1/50 slope condition (DS-224 and DS-502) in the CLASH datasets.

In the procedure to formulate IFORM, the uncertainty of model prediction may arise in the two processes mentioned in the previous section; (a) the estimation of overtopping based on predicted runup (or deficit in freeboard) and (b) the prediction of runup level from the specified wave and installation condition. Note that the influence of the uncertainty in runup estimation appears in both of them. The present study focuses on the former one (corresponding to the part in the square brackets in Eq. (30)), and the relation between the predicted runup and

overtopping discharge is properly described for a wide range of conditions in the refined IFORM. Accordingly, the underestimation observed here may be resulted from the latter one, namely the underestimation of maximum wave runup. The runup formula used in IFORM is based on the experiments conducted for 1/10 to 1/30 slope of the seabed by Mase et al. (2004) and by Mase et al. (2013). Over the conditions covered in these experiments, the runup formula (Eq. (4)) has been validated to be sufficiently accurate as shown in Fig. 10 in Mase et al. (2013). Since the tendency of underestimation in overtopping discharge is observed for the mildly sloping bed with slope <1/30 (out of the conditions of Mase et al. (2004) and Mase et al. (2013)), additional confirmations may be needed. Preliminary examinations indicated that the runup prediction based on Eq. (4) is lower than the prediction based on the method by Altomare et al. (2016) for DS-168. Besides, the general features of the influence of smaller prediction in runup height on overtopping discharge can be inferred from Fig. 7. The sensitivity of the overtopping prediction to the estimation of runup as well as imaginary slope and breaking depth deserves further investigation, but it is beyond the scope of this paper. These aspects will be treated in the future study.

7. Summary remarks

This study attempted to optimize the Integrated Formula of Overtopping and Runup Modeling (IFORM) for mean overtopping discharge to achieve a high-performance assessment for a broader range of overtopping conditions. For this purpose, the regression formula between the overtopping discharge and the runup in IFORM was re-examined and re-evaluated. The formulation has been reconstructed with a set of piecewise formulas for three ranges of the runup level relative to the freeboard. The refined formulas retain the high performance of the original IFORM in the range where the freeboard of the seawall is relatively low, while they improve the tendency of underestimation selectively in the range of relatively high freeboard conditions close to the threshold of overtopping occurrence.

The prediction capability of the refined IFORM for overtopping discharge was validated by comparison with various existing hydraulic experiments. For gently sloped seawalls installed at shallow depth or on land, the model predictions were compared with the experiment by Tamada et al. (2002). The results indicated that the refined IFORM is able to well reproduce the experimental observations over a broader range of overtopping conditions and that it enhances the quantitative accuracy of the prediction. The model predictions were further compared with the experiments that were conducted independently from the establishment of IFORM. For inclined seawall installed at shallow water depth, the model prediction was compared with the measurement by Altomare et al. (2016). The model performance of the refined IFORM was shown to be comparable as that of the Altomare model (EurOtop2018 model) that is tuned for the particular experiment. The prediction accuracy of the refined IFORM was superior to the Goda formula. For plain vertical seawalls, the model predictions were compared with the data extracted from the original CLASH datasets. The results well demonstrated the enhanced applicability of the refined IFORM. The model capability was shown to be as good as those of the existing representative models such as those proposed by EurOtop (2018) and Goda (2009b). Finally, an alternative form of the scaling of the overtopping discharge was provided and discussion has been made on a novel strategy to develop an overtopping model.

CRediT authorship contribution statement

Masatoshi Yuhi: Conceptualization, Methodology, Investigation, Formal analysis, Writing - original draft. **Hajime Mase:** Conceptualization, Supervision, Writing - review & editing, Funding acquisition. **Sooyoul Kim:** Writing - review & editing, Funding acquisition. **Shinya Umeda:** Investigation, Writing - review & editing. **Corrado Altomare:** Investigation, Writing - review & editing, Funding acquisition.

Declaration of competing interest

The authors declare that they have no known competing financial interests or personal relationships that could have appeared to influence the work reported in this paper.

Acknowledgements

This work is partially supported by the Grants-in-Aid for Scientific Research by the Japan Society for the Promotion of Science [Grant No. 19H02403 and 20K05046] and the collaborative research program of the Disaster Prevention Research Institute of Kyoto University [Grant No. 30G-09]. Dr. C. Altomare acknowledges funding from the European Union's Horizon 2020 research and innovation programme under the Marie Sklodowska-Curie grant agreement No.: 792370. Suggestive comments from Prof. Hiraishi (Kyoto University), Dr. Kawasaki and Dr. Mizutani (Hydro Technology Institute Co., Ltd.) are most appreciated. Assistance rendered by Mr. Ohtani (a former student of Kanazawa University) and Ms. Ichimura (graduate student of Kanazawa University) is acknowledged. Constructive comments and suggestions from the anonymous reviewers are appreciated.

References

Altomare, C., Suzuki, T., Chen, X., Verwaest, T., Kortenhaus, A., 2016. Wave overtopping of sea dikes with very shallow foreshores. Coast. Eng. 116, 236–257.

Altomare, C., Suzuki, T., Peeters, P., Mostaert, F., 2017. Empirical Overtopping Law for Very Shallow Foreshores, Final Report. Ver. 2.0. FHR Reports, 13_116_1. Flanders Hydraulics Research, Antwerp, Belgium.

Altomare, C., Berardi, L., Mase, H., Gironella, X., 2020. Determination of semi-empirical models for mean wave overtopping using an evolutionary polynomial paradigm. J. Mar. Sci. Eng. 8, 570.

Chen, X., Hofland, B., Altomare, C., Suzuki, T., Uijttewal, W., 2015. Forces on a vertical wall on a dike crest due to overtopping flow. Coast. Eng. 95, 94–104.

Coastal Development Institute of Technology (CDIT), 2018. The Technical Standards and Commentaries for Coastal Facilities in Japan, revised edition. The Ports and Harbours Association of Japan (in Japanese).

Coastal Engineering Committee, Japan Society of Civil Engineers (JSCE), 2004. Design Manual for Coastal Facilities 2000. Maruzen Co. Ltd., Tokyo, p. 577.

De Rouck, J., Van der Meer, J.W., Allsop, N.W.H., Franco, L., Verhaeghe, H., 2002. Wave overtopping at coastal structures: development of a database toward up-graded prediction model. Proc. 28th Int. Conf. Coast. Eng., ASCE 2140–2152.

EurOtop, 2007. In: Pullen, T., Allsop, N.W.H., Kortenhaus, A., Schüttrumpf, H., Van der Meer, J.W. (Eds.), Wave Overtopping of Sea Defenses and Related Structures: Assessment Manual. www.overtopping-manual.com.

EurOtop, 2018. In: Van der Meer, J.W., Allsop, N.W.H., Bruce, T., De Rouck, J., Kortenhaus, A., Pullen, T., Schüttrumpf, H., Troch, P., Zanuttigh, B. (Eds.), Manual on Wave Overtopping of Sea Defenses and Related Structures. An Overtopping Manual Largely Based on European Research, but for Worldwide Application. www.overtopping-manual.com.

Goda, Y., 2004. Random Seas and Design of Maritime Structure, second ed. World Scientific.

Goda, Y., 2009a. A performance test of nearshore wave height prediction with CLASH datasets. Coast. Eng. 56, 220–229.

Goda, Y., 2009b. Derivation of unified wave overtopping formulas for seawalls with smooth, impermeable surfaces based on selected CLASH datasets. Coast. Eng. 56, 385–399.

Hedges, T.S., Reis, M.T., 1998. Random wave overtopping of simple sea walls: a new regression model. Proc. Inst. Civil Eng., Water, Marit. & Energy 130 (1), 1–10.

Hunt, I.A., 1959. Design of seawalls and breakwaters. Proc. Am. Soc. Civ. Eng. 85, 123–152.

Ibrahim, M.S.I., Baldock, T.E., 2020. Swash overtopping on plane beaches – reconciling empirical and theoretical scaling laws using the volume flux. Coast Eng. 157, 103668.

Liu, Y., Li, S., Chen, S., Hu, C., Fan, Z., Jin, R., 2020. Random wave overtopping of vertical seawalls on coral reefs. Appl. Ocean Res. 100, 102166.

Mase, H., Kirby, J.T., 1993. Hybrid frequency-domain KdV equation for random wave transformation. Proc. 23rd Int. Conf. Coast. Eng., ASCE. 474–487.

Mase, H., Miyahira, A., Hedges, T.S., 2004. Random wave run-up on seawalls near shorelines with and without artificial reefs. Coast Eng. J. 46 (3), 247–268.

Mase, H., Tamada, T., Yasuda, T., Hedges, T., Reis, M., 2013. Wave runup and overtopping at seawalls built on land and in very shallow water. J. Waterw., Port., Coast., Ocean Eng. 139 (5), 346–357.

Mase, H., Tamada, T., Yasuda, T., Kawasaki, K., 2016. Integrated formula of wave overtopping and runup modeling for seawalls. J. JSCE, Ser. B2 (Coastal Eng.) 72 (1), 83–88 (in Japanese).

Nakamura, M., Sasaki, Y., Yamada, J., 1972. Runup on seawalls with composite cross section. Proc. of Coast. Eng., JSCE. 19, 309–312 (in Japanese).

Reis, M.T., Hu, K., Hedges, T.S., Mase, H., 2008. A comparison of empirical semiempirical, and numerical wave overtopping models. J. Coast Res. 24 (2B), 250–262.
Tamada, T., Inoue, M., Tezuka, T., 2002. Diagrams for the estimation of wave overtopping rate on gentle slope-type seawalls. Proc. Coast. Eng., JSCE. 49, 641–645 (in Japanese).
Tamada, T., Mase, H., Yasuda, T., 2015. Wave runup and overtopping integrated model for vertical seawall based on CLASH datasets. Proc. SCACR2015, Int. Short Course/ Conf. on applied Coast. Res. 361–370.
Technical Advisory Committee on Flood Defense (TAW), 2002. In: Van der Meer, J.W. (Ed.), Technical Report Wave Run-Up and Wave Overtopping at Dikes. TAW, Delft, The Netherlands.
The Overseas Coastal Area Development Institute of Japan (OCDI), 2009. Technical Standards and Commentaries for Port and Harbour Facilities in Japan. OCDI, Tokyo.
Van der Meer, J.W., Verhaeghe, H., Steendam, G.J., 2009. The new wave overtopping database for coastal structures. Coast. Eng. 56, 108–120.
U.S. Army Corps of Engineers (USACE), 2002. In: Coastal Engineering Manual (CEM), EM 1110-2-1100. USACE, Washington, D.C.
Van der Meer, J.W., Bruce, T., 2014. New physical insights and design formulas on wave overtopping at sloping and vertical structures. J. Waterw. Port, Coast. Ocean Eng. 140, 04014025-1-04014025-18.
Van Gent, M.R.A., 1999. Physical Model Investigations on Coastal Structures with Shallow Foreshores: 2D Model Tests with Single and Double-Peaked Wave Energy Spectra. Delft Hydraulics/Waterbouwkundig Labratorium.
Verhaeghe, H., 2005. Neural Network Prediction of Wave Overtopping at Coastal Structure. Doctorate Dissertation at Dep. Civil Eng.. Ghent University.